Original Research Article

Comparative Evaluation of Seismic Resistance, Damping, and Base Isolation under Earthquake Loading Using 3D-Printed Building Models

Donggyu Han and Priya Thambaje Gopalan

SEK International School Qatar, Al Farouq Street, Zone 65, Onaiza District, P.O. Box 19716, Doha, Qatar

ABSTRACT

This study investigates the effectiveness of different seismic design strategies in improving the earthquake resilience of buildings. Motivated by the 2011 Tohoku earthquake in Japan, the research focuses on three major seismic systems: seismic resistance, seismic damping, and seismic base isolation. Seismic resistance enhances structural strength to withstand forces, seismic damping dissipates energy through mechanisms such as dampers, and base isolation reduces energy transfer by separating the building from the ground. An experimental approach was used involving 3D-printed building models equipped with each system. Measurements of wave amplitude and displacement were recorded to assess performance under simulated seismic activity. Results indicated that seismic damping was most effective in reducing wave amplitude, while base isolation minimized displacement. Seismic resistance was the most economical but least effective in mitigating energy. The findings highlight the importance of selecting seismic designs based on building context while balancing safety and cost. Limitations include the small experimental scale and simplified simulation conditions, suggesting the need for further research under more realistic scenarios.

Keywords: Seismic design; Earthquake engineering; Base isolation; Damping systems; Structural resilience; Architecture; Vibration analysis

INTRODUCTION

The 2011 Tohoku earthquake in Japan resulted in 19,759 deaths and left 2,553 people missing (1), highlighting the devastating impact that earthquakes have on communities. Such events emphasize the need for effective seismic design strategies to enhance structural safety.

Earthquakes occur through the release of elastic potential energy stored at colliding tectonic plates, which is converted into seismic energy and released through seismic waves (2). Body waves (P-waves and S-waves) travel through the interior of the Earth and arrive first, while surface waves (Love waves and Rayleigh waves) travel along the surface (3-5). The velocities of these waves are directly related to the applied force.

$$v \propto \frac{1}{\lambda} \propto f \propto E \propto F$$

Corresponding author: Priya Thambaje Gopalan, E-mail: priya.gopalan@sek.qa; Donggyu Han, E-mail: dinggyu922@gmail.com.

Accepted August 20, 2026
https://doi.org/10.70251/HYJR2348.4413631371

(Equation 1. Proportionality between wave velocity and force)

V represents the velocity of the wave; λ represents wavelength; f represents frequency; E represents energy dissipated; F represents the applied force.

Since wave velocity is proportional to frequency, while frequency is also related to energy and force, faster wave velocities signify a stronger force applied to buildings. In addition, Love waves shake structures with a horizontal shearing motion, while Rayleigh waves move the ground in an elliptical motion, which tilts the building foundation. These waves generate lateral and vertical stresses in buildings during an earthquake (6).

A building responds to earthquakes according to its natural frequency. When the building's natural frequency matches the frequency of seismic surface waves, resonance occurs and the oscillation amplitude is maximized. As a result, the risk of structural failure increases as the building responds to inertial effects.

$$f_{natural} = \frac{1}{2\pi} \times \sqrt{\frac{k}{m}}$$

(Equation 2. Natural Frequency Formula)

k represents the stiffness of the structure (N/m), and m represents the mass of the structure (kg). Seismic design strategies aim to prevent the collapse of buildings. However, the mechanisms used to prevent collapse differ according to their fundamental principles. These strategies depend on structural dynamics, energy dissipation, or isolation of the building from the ground.

Primarily, a seismic resistance system increases the strength and stiffness of structural materials through structural design (Figure 1). Reinforcement bars are added to concrete to compensate for its low tensile strength. Shear walls are also added to transfer lateral loads to the foundation. In practice, the Imperial Hotel in Tokyo demonstrated the effectiveness of this approach during the 1923 earthquake in Japan. As this system focuses on stabilizing the structure without active control, it is considered a passive system (7, 8).

Furthermore, a seismic damping system reduces earthquake impacts through energy dissipation (Figure 2). With the addition of supplementary elements such as fluid dampers or tuned mass dampers, the system dissipates seismic energy and can also control the natural frequency through the addition of mass. This approach is used in Taipei 101, where it reduces building vibration (9).

A base isolation system focuses on isolating the building foundation from the ground (Figure 3). With sliding or elastomeric bearings under the foundation, it isolates the structure from earthquake-induced ground motion. Each bearing helps stabilize the building against lateral forces. As a result, less seismic energy is transferred into the building. This system is currently used in Los Angeles City Hall (10, 11).

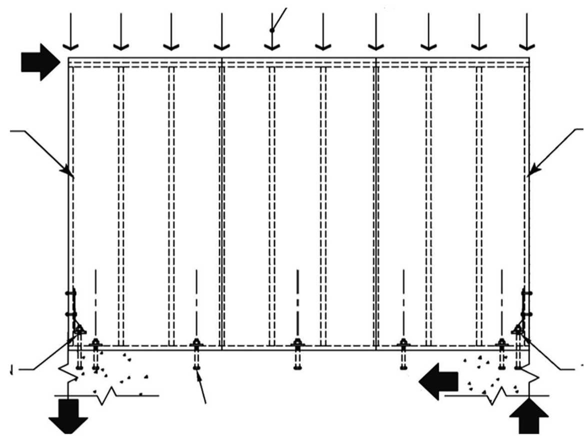

Figure 1. *Shear wall subjected to earthquake-induced lateral loading, illustrating how the wall resists in-plane seismic forces and transfers the resulting shear and overturning actions to the foundation. Reproduced from FEMA P-50-1 (7).*

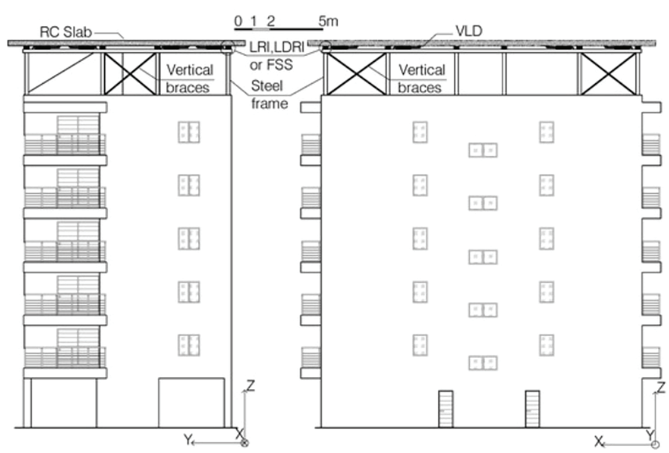

Figure 2. *Elevation of a reinforced-concrete building equipped with a tuned mass damper (TMD) at the top of the structure for reducing structural response under seismic excitation. Reproduced from Reggio et al. (8) under the Creative Commons Attribution 4.0 International (CC BY 4.0) license.*

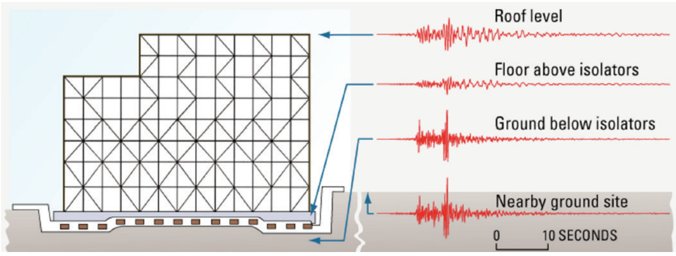

Figure 3. *Schematic cross-section of a base-isolated building showing isolation bearings positioned between the building and foundation to reduce the transmission of ground motion to the structure. Reproduced from the U.S. Geological Survey (USGS); public domain (10).*

These three strategies address earthquake impacts differently. They also have different cost implications, with seismic resistance being the most economical and base isolation being the most expensive to implement. Therefore, this study used 3D-printed building models to investigate the following question: to what extent do seismic resistance, seismic damping, and base isolation systems differ in wave amplitude and displacement under simulated seismic loading? It was hypothesized that both damping and base isolation systems would outperform the resistance system in reducing wave amplitude and displacement. Because these two systems approach earthquakes through energy dissipation and isolation, they were expected to outperform seismic resistance systems, which passively resist earthquake-induced forces.

METHODS AND MATERIALS

The materials used in this experiment included a 3D-printed building model with empty central space, a 3D-printed model with a damping hanger, a 3D-printed base-isolation component, a 3D-printed base plate, string and tape, a small ball, four vibration generators, two power supplies, and two stands.

To prepare for the experiment, a 120 mm × 120 mm × 15 mm plate with an 82.5 mm × 82.5 mm × 12.5 mm square hole in the middle was 3D-printed. At each of the four corners, a circular hole with a diameter of 9.5 mm was created to attach the plate to the vibration generators.

Three 3D-printed building models were produced with identical dimensions (80 mm × 80 mm × 145 mm) and material (PLA filament). A rectangular opening was created in the middle section of each model above 30 mm to leave the interior empty. At the top, a circular hole with a diameter of 72 mm and a depth of 30 mm was created to provide space for the ball to move during the experiment. After the three models were printed, a 100 mm string was attached to the middle of each model for wave-amplitude measurement.

For the seismic damping model, an additional ring was attached to the model to hold four 20 g masses that functioned as a tuned mass damper. For the base isolation system, a rubber-band bearing was attached between the model and the plate to function as an isolation bearing.

After preparation of the models to work as buildings in the experiment, the set-up process began. The base plate was attached to four Philip Harris Vibration Generators (Findel International, product code E8H30701; frequency range D.C.–10 kHz, max peak-to-peak displacement 8 mm at 1 Hz decreasing with frequency, coil impedance 3.5 Ω at 50 Hz, max carrying load 150 g), driven by two power generators set to 8 V. Outputs were compared on the oscilloscope beforehand to confirm consistency; no further adjustment was needed. Each seismic design model was placed on the plate in turn, with a pickup transducer taped in-line with the string to sense wave amplitude, recorded on an OWON SDS1022 digital oscilloscope (Findel International; dual-channel, 20 MHz, 100 MSa/s, 10 kpts). Channel 1 captured the amplitude signal; Channel 2 recorded a reference signal from the generator drive line. For each trial, the generator was activated and released, and peak-to-peak amplitude was read from the resulting decay trace. Ball displacement was recorded as the maximum lateral distance it moved from rest during the same window. A small ball was positioned at the centre of the top cavity to measure maximum lateral displacement during vibration, and the model and experimental setup are shown in Figures 4 and 5.

Real-life conversion into experiment

The primary aim of the experimental setup was to simulate earthquake-induced vibration. A plate holding the 3D-printed buildings was created for this purpose, and vibration generators were used to transfer vibrational energy through the plate in a manner intended to simulate earthquake ground motion. Each design was then represented using a specific principle. For seismic resistance, structural reinforcement was represented by adding glue to the structure to act as shear-wall-type reinforcement. For seismic damping, a hanging heavy-mass system was used by adding heavy blocks to the model. For seismic isolation, an elastomeric-bearing concept was represented by placing glass-like plates

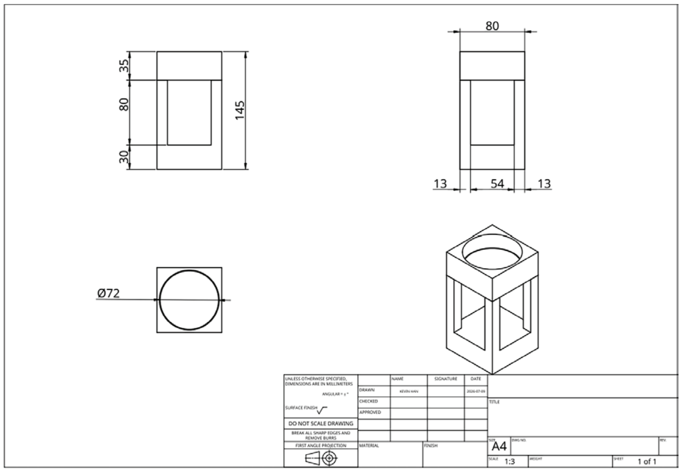

Figure 4. *Building Model Blueprint with Measurements.*

Figure 5. *Apparatus of the experiment with Printed Building Models.*

between the base and the building to create a low-friction bearing. These approaches were selected to represent principles used in real seismic design. Furthermore, the ball was placed at the top of the building to observe how oscillation affected an object within the model.

Variables

The independent variable was the type of seismic design system (seismic resistance, seismic damping, and base isolation). The dependent variables were the maximum wave amplitude recorded on the building model and the maximum displacement of the ball at the top of the model. Controlled variables included the power supplied to the vibration generators (fixed at 8 V), the printing material (PLA), the 3D printer used, and the ball and string used for measurement.

Independent Variable: Types of Seismic Designs

This investigation examined how different types of seismic designs affected the stability of the building models under simulated earthquake conditions. Three similar building structures were produced using the same 3D printer. However, each seismic design had its own distinguishing feature. The resistance model used glue on the exterior to represent shear-wall-type reinforcement; the damping model used a hanging heavy mass; and the isolation model used a rubber band as a bearing between the building and foundation base.

Dependent Variable 1: Wave Amplitude of the String Attached to the Building Model

Wave amplitude was used to measure the oscillatory response of the building model. A string was attached to the wall of the building model, and a sensor was used to record its wave amplitude during vibration. These measurements were used to compare how the three seismic systems responded under the same experimental conditions.

Dependent Variable 2: Displacement of the Ball at the Top of the Model

The small ball at the top of the model was used to indicate how strongly the building shook and to represent the movement that occupants might experience. A cavity was created at the top of the building model, allowing the ball to move laterally during vibration. The maximum lateral displacement of the ball was recorded.

Controlled Variable 1: Power of Vibration

In this experimental setup, vibration power represented the input used to simulate seismic excitation. Variation in power could have affected the results independently of the different seismic designs. Therefore, the 3D-printed plate was connected to four vibration generators powered by two power supplies, and the power supplies were fixed at 8 V throughout the experiment.

Controlled Variable 2: 3D-Printed Building Material

The same material was used for all 3D-printed building models because differences in material properties could have affected the dependent variables. PLA was used for all three designs, and all models were printed using the same 3D printer.

Controlled Variable 3: Ball and String Used in the Experiment

The same ball and string were used throughout the experiment because differences in surface friction or string properties could have affected the measurements. The same 3D-printed ball and the same type and length of string were therefore used for all three structures.

Procedure

The base plate was mounted on the four vibration generators, which were connected to two power supplies fixed at 8 V. Each building model was then placed on the base plate in turn, with a wave amplitude sensor attached to the model's string and a ball positioned in the top cavity. A motion detector was positioned above the model to measure its maximum displacement. The vibration generators were then activated, and the largest wave amplitude and maximum ball displacement were recorded for that trial. This process was repeated for each model, with five trials conducted per model to reduce measurement uncertainty.

Statistical Method

For each seismic design system, the mean and standard deviation of each measurement were calculated. Analysis of variance (ANOVA) was used to evaluate overall differences in mean wave amplitude and mean displacement among the three seismic design systems. A significance threshold of $\alpha = 0.05$ was used. F-statistics, degrees of freedom, and p-values were reported for each analysis. When a significant difference was found ($p < 0.05$), Tukey's HSD test was used to determine which specific systems differed from one another. Results are presented as mean ± standard deviation (SD), calculated from five independent trials for each seismic design system.

RESULTS

The seismic resistance system produced the highest mean wave amplitude (15.6 ± 1.70 mm), followed by the base isolation system (7.71 ± 1.21 mm) and the seismic damping system (5.17 ± 0.93 mm) (Tables 1 and 3; Figure 6). A one-way ANOVA showed a significant difference among the three systems, $F(2, 12) = 84.15$, $p = 8.69 \times 10^{-8}$. Tukey HSD testing showed significant differences between resistance and damping ($p < 0.001$), resistance and base isolation ($p < 0.001$), and damping and base isolation ($p = 0.026$).

For maximum ball displacement, the seismic resistance system also showed the highest mean value (2.96 ± 0.18 cm), whereas the seismic damping and base isolation systems showed lower values of 0.65 ± 0.13 cm and 0.41 ± 0.08 cm, respectively (Tables 2 and 3;

Table 1. *Peak-to-peak wave amplitude measured for each seismic design system across five trials. Individual measurements are reported in millimetres (mm), with a measurement uncertainty of ±0.05 mm. Summary values are reported as mean ± standard deviation (SD), where SD represents variability among the five trials.*

Amplitude of Oscillation (mm)	Largest Wave Amplitude (mm) ± 0.05 mm				
	Trial 1	Trial 2	Trial 3	Trial 4	Trial 5
Seismic Resistance System	13.25	16.89	14.52	15.71	17.38
Seismic Damping System	5.12	4.67	6.33	5.80	3.95
Base Isolation System	7.23	8.44	6.62	9.46	6.79

Table 2. *Maximum lateral displacement of the ball measured for each seismic design system across five trials. Individual measurements are reported in centimetres (cm), with a measurement uncertainty of ±0.05 cm. Summary values are reported as mean ± standard deviation (SD), where SD represents variability among the five trials.*

Displacement of the ball (cm)	Maximum Displacement (cm) ± 0.05 cm				
	Trial 1	Trial 2	Trial 3	Trial 4	Trial 5
Seismic Resistance System	2.72	3.19	2.94	2.89	3.07
Seismic Damping System	0.75	0.49	0.63	0.80	0.58
Base Isolation System	0.50	0.34	0.42	0.31	0.47

Figure 7). The difference among the three systems was significant, $F(2, 12) = 547.20$, $p = 1.63 \times 10^{-12}$. Tukey HSD testing showed significant differences between resistance and damping ($p < 0.001$), resistance and base isolation ($p < 0.001$), and damping and base isolation ($p = 0.037$).

Table 3. Summary of mean wave amplitude and maximum lateral ball displacement for the three seismic design systems. Values are reported as mean ± standard deviation (SD) from five independent trials (n = 5). Wave amplitude is reported in mm and displacement in cm.

Types of Design	Wave Amplitude (mm)	Displacement (cm)
Seismic Resistance System	15.6 ± 1.70	2.96 ± 0.18
Seismic Damping System	5.17 ± 0.93	0.65 ± 0.13
Base Isolation System	7.71 ± 1.21	0.41 ± 0.08

Sample Calculation

$\bar{x}_{\text{millimetre}}$ of Amplitude of Oscillation for Seismic Resistance System

$$\bar{x} = \frac{\Sigma \text{ all trials}}{\text{Number of trials}}$$

Mean Formula

Mean Amplitude of Oscillation in Wave

$$\bar{x} = \frac{\{(13.25 \pm 0.05) + (16.89 \pm 0.05) + (14.52 \pm 0.05)\}}{5} + \frac{\{(15.71 \pm 0.05) + (17.38 \pm 0.05)\}}{5}$$

$$\bar{x} = 15.55 \approx 15.6$$

Mean Displacement of Ball

$$\bar{x} = \frac{\{(2.72 \pm 0.05) + (3.19 \pm 0.05) + (2.94 \pm 0.05)\}}{5} + \frac{\{(2.89 \pm 0.05) + (3.07 \pm 0.05)\}}{5}$$

$$\bar{x} = 2.962 \approx 2.96$$

Mean Uncertainty of Amplitude of Oscillation

$$\pm = \frac{\{0.05 \times 5\}}{5}$$

$$\bar{x}_{milliemetre} = 15.6 \pm 0.05$$

Mean Uncertainty of Displacement of Ball

$$\pm = \frac{\{0.05 \times 5\}}{5}$$

$$\bar{x}_{centimetre} = 2.96 \pm 0.05$$

Graphs

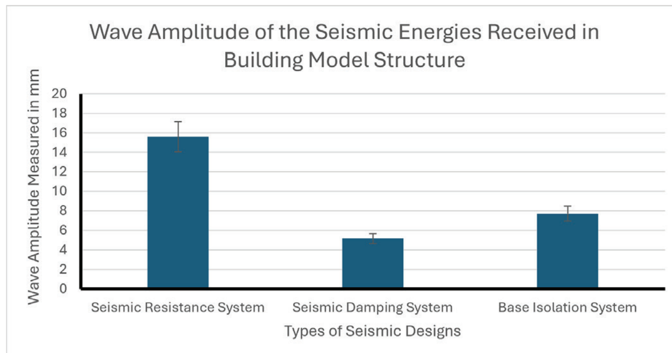

Figure 6. *Mean wave amplitudes measured from the string attached to each building model under identical vibration-generator conditions. Error bars represent ±1 standard deviation from five trials. Lower wave amplitude indicates a lower measured oscillatory response of the building model.*

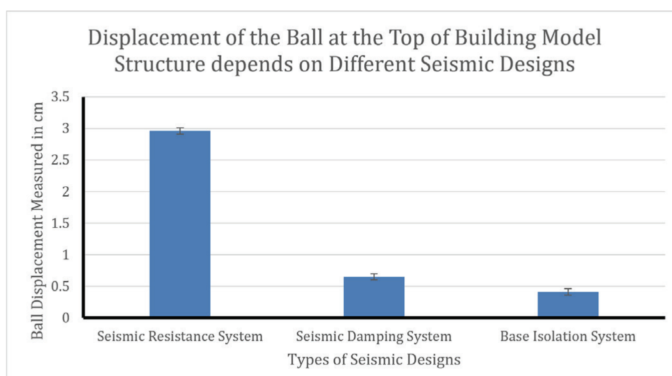

Figure 7. *Mean maximum lateral displacement of the ball at the top of each building model under identical vibration-generator conditions. Error bars represent ±1 standard deviation from five trials. Lower displacement indicates less measured lateral movement of the model during vibration.*

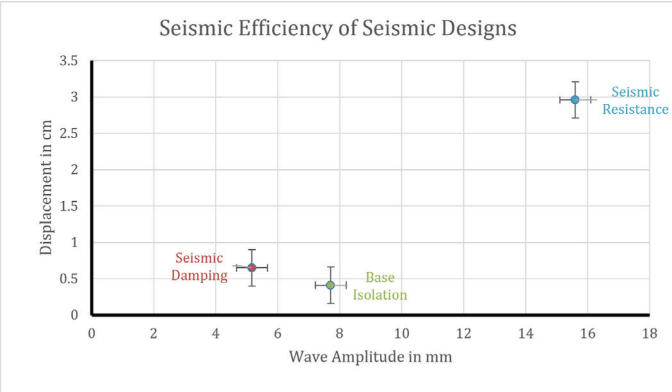

Figure 8. *Comparison of mean wave amplitude and mean maximum lateral ball displacement for the three seismic design systems. Lower values on both axes indicate a lower measured response under the experimental conditions; therefore, points closer to the bottom-left corner represent lower combined wave amplitude and displacement.*

DISCUSSION

Considering the scale and conditions of this experiment, the seismic damping and base isolation systems were the most effective in reducing transmitted wave amplitude and ball displacement. The seismic resistance system showed the largest measured response, as shown in the graphs. While the damping and isolation systems showed comparatively lower displacement and wave amplitude, the resistance system showed a greater structural response under the experimental conditions. In Figure 8, the damping and isolation systems were positioned closer to the lower-left region because they produced lower displacement and wave-amplitude values. This pattern was consistent throughout the experiment and was consistent with the mechanisms described in the Introduction. Damping dissipates energy, while isolation limits the transmission of seismic motion; in contrast, the resistance system relies on passive structural reinforcement.

Table 1 shows that the Seismic Resistance System had the highest wave-amplitude values, while the Seismic Damping and Base Isolation Systems had noticeably lower values. The displacement results in Table 2 show a similar pattern, with the Seismic Resistance System producing the greatest displacement. This is also visible in Figures 6 and 7, where the Seismic Resistance System bars are substantially taller than those of the other two systems. The statistical analyses reported in the Results confirmed that the seismic design system significantly influenced both measured wave amplitude and maximum ball displacement. The Tukey HSD comparisons further identified which specific seismic design systems differed significantly from one another.

These results also align with findings in the structural engineering literature. Both dampers and base isolation have been shown to reduce structural response compared with unprotected structures, with larger reductions observed when the two systems were combined rather than used individually (12). Although installing both systems can substantially increase construction costs, their combined use may be considered when greater structural protection is required (13). The current experiment did not test a combined system, so its effectiveness cannot be determined from these experimental results. However, the cited literature suggests that combining the systems has the potential to further reduce structural response.

Furthermore, depending on the priority of the seismic design, the two systems (seismic damping and base isolation) may be applied differently. Base isolation may be preferable when minimizing occupant displacement is a priority. On the other hand, damping may be more appropriate when reducing the measured oscillatory response is the main priority, as indicated by the experimental results (14).

The cited peer-reviewed study investigated the combination of two control strategies: base isolation and seismic mass dampers. Through numerical analysis across multiple seismic ground motions, the authors reported that the damping system alone produced up to an approximately 20% response reduction, base isolation alone produced approximately a 70% reduction, and the combined system achieved more than an 80% reduction in structural response (14).

The cost-effectiveness discussed earlier should be treated as an additional consideration rather than the primary criterion for seismic design. Protection against earthquake impacts should remain the main priority in architectural and structural design.

CONCLUSION

In this study, the effectiveness of seismic resistance, seismic damping, and base isolation systems was compared using 3D-printed building models under simulated earthquake conditions. As shown in the graphs, seismic damping produced the greatest reduction in wave amplitude, while base isolation produced the lowest displacement. Both systems significantly outperformed the seismic resistance system. As discussed, these two systems could also be considered in combination. If construction costs become too high, the design decision may instead prioritize either occupant displacement or reduction of the structural response.

Because the experiment used simplified, small-scale models, the findings should be interpreted within the experimental conditions. Future research should test the systems at a larger scale and examine combined seismic design strategies.

One of the biggest limitations was the scale of the experiment. The experiment was conducted using resources available at school, so a full shaking table or other realistic earthquake-simulation equipment could not be used. The building models were also only 8 cm in size, which is much smaller than real buildings. This scale difference may have affected the behavior of the models and introduced factors that would be less important at full scale. A larger experimental setup with a controlled moving platform would provide a more realistic representation of structural response.

Another limitation was the limited variation in seismic power. The vibration generators were limited to an input of 8 V, which restricted the range of excitation applied to the models. As a result, the experiment could not examine how the three seismic systems behaved under a wider range of vibration intensities. Future testing with higher-capacity vibration equipment or a controllable shaking platform would allow the structural response to be examined under more varied loading conditions.

Finally, another limitation was the simplified nature of the seismic models. Each model represented one seismic design strategy independently, whereas real buildings may combine several strategies, such as shear walls, damping devices, and base-isolation bearings. Therefore, the experiment does not show how these systems would interact when used together. Testing combined systems in future experiments would allow a more realistic comparison and could determine whether their combined use further reduces structural response.

ACKNOWLEDGEMENTS

I would like to express my sincere gratitude to our Head of School, Dr. María Paz Aguilera Gamero, for providing me with the opportunity and platform to conduct my work effectively. I am also deeply thankful to Mr. Kim Derudder for his continuous guidance, support, and encouragement throughout this journey. My heartfelt appreciation goes to my parents and teachers for their faith in me, their trust in my abilities, and their constant support of my hard work and dedication.

CONFLICT OF INTEREST

The author declares that there are no conflicts of interest related to this work.

REFERENCES

1. Wei Y, Chamberlin C. Modeling of the 2011 Japan tsunami: lessons for near-field forecast. *Pure Appl Geophys*. 2012; 169 (9): 1583-1599. Available from: https://link.springer.com/article/10.1007/s00024-012-0519-z [cited 2024 Nov 12].
2. Lu K, Cao Z, Hou M, Jiang Z, Shen R, Wang Q, Sun G, Liu J. The mechanism of earthquake. *Int J Mod Phys B*. 2018; 32 (7): 1850080. Available from: https://doi.org/10.1142/S0217979218500807 [cited 2024 Oct 14]
3. Pieri DC, Melis AM. Seismic waves. In: ScienceDirect Topics [Internet]. Amsterdam: Elsevier; 2007. Available from: https://www.sciencedirect.com/topics/physics-and-astronomy/seismic-waves [cited 2024 Oct 8].
4. Michigan Technological University. Surface waves [Internet]. Houghton (MI): Michigan Technological University. Available from: https://www.mtu.edu/geo/community/seismology/learn/seismology-study/surface-wave/ [cited 2024 Oct 10].
5. Maranò S, Fäh D. Processing of translational and rotational motions of surface waves: performance analysis and applications to single sensor and to array measurements. *Geophys J Int*. 2014; 196 (1): 317-331. Available from: https://academic.oup.com/gji/article/196/1/317/584783 [cited 2026 Aug 18]. https://doi.org/10.1093/gji/ggt187
6. Naaman AE. Reinforced concrete. In: ScienceDirect Topics [Internet]. Amsterdam: Elsevier; 2001. Available from: https://www.sciencedirect.com/topics/agricultural-and-biological-sciences/reinforced-concrete [cited 2024 Sep 20].
7. Federal Emergency Management Agency. Seismic retrofit guidelines. FEMA P-50-1. Washington, DC: FEMA; 2021. Available from: https://www.fema.gov/sites/default/files/documents/fema_p-50-1-seismic-retrofit-guidelines-8252021.pdf [cited 2026 Aug 18].
8. Reggio A, Restuccia L, Martelli L, Ferro GA. Effectiveness of tuned mass damper in reducing damage caused by strong earthquake in a medium-rise building. *Appl Sci*. 2023; 13 (11): 6815. doi:10.3390/app13116815. Available from: https://www.mdpi.com/2076-3417/13/11/6815 [cited 2026 Aug 18]. https://doi.

org/10.3390/app13116815
9. Federal Emergency Management Agency. Earthquake-resistant design concepts. FEMA P-749. Washington, DC: FEMA; 2022. Available from: https://www.fema.gov/sites/default/files/documents/fema_p-749-earthquake-resistant-design-concepts_112022.pdf [cited 2026 Aug 18].
10. U.S. Geological Survey. Evaluating earthquake protection [Internet]. Reston (VA): U.S. Geological Survey; 2003 [cited 2026 Aug 18]. Available from: https://pubs.usgs.gov/fs/2003/fs068-03/eval.html.
11. Thakur R, Tiwary AK. Seismic response of base-isolated RC frame structure with various isolators under near-fault ground motion. Innov Infrastruct Solutions [Internet]. 2023 8(11):298. Available from: https://link.springer.com/article/10.1007/s41062-023-01229-z [cited 2026 Jul 9]
12. Al-Janabi MAQ, Al-Jeznawi D, Yang TY, Bernardo LFA, Andrade JMA. Enhancing structural resilience for sustainable infrastructure: a global review of seismic isolation and energy dissipation practices. Sustainability [Internet]. 2025; 17 (16): 7314. Available from: https://www.mdpi.com/2071-1050/17/16/7314 [cited 2026 Jul 9]. https://doi.org/10.3390/su17167314
13. Naderpour H, Naji N, Burkacki D, Jankowski R. Seismic response of high-rise buildings equipped with base isolation and non-traditional tuned mass dampers. *Appl Sci*. 2019; 9 (6): 1201. doi:10.3390/app9061201. Available from https://www.mdpi.com/2076-3417/9/6/1201 [cited 2026 Aug 5]. https://doi.org/10.3390/app9061201